  Bull. Chem. Soc. Jpn., 65, 3462—3469 (1992) [Vol. 65, No. 12

Adsorption-Induced Electrical Conductivity of Some Ferrocene Derivatives: Rates of Adsorption and Desorption of Vapors

Ashis BHATTACHARJEE and Biswanath MALLIK*
Department of Spectroscopy, Indian Association for the Cultivation of Science,
Jadavpur, Calcutta-32, India
(Received April 28, 1992)

The change in dark conductivity of some ferrocene derivatives on adsorption of some organic solvent has been studied in sandwich cell configurations at different cell temperatures. Appreciable enhancements in the dark conductivity are observed. Such enhancement depends on the amount of adsorbed vapor, cell temperature as well as the chemical nature of the adsorbate. The sensitivity towards a vapor is also found to vary depending on the nature of the substituent groups in the ferrocene ring. Both the adsorption and desorption rates follow the modified Roginsky–Zeldovich equation. The temperature dependence and the nature of the solid–vapor interaction have been deduced from the rate data analysis.

In our earlier communications[1,2] we have discussed about the unusual changes in the electrical conductivity of ferrocene (Fc–H) and some of its derivatives upon adsorption of some solvent vapors. A conductivity peak was observed in the plot of the measured dark current vs. cell temperature for a sandwich cell of any of these materials with adsorbed vapors. The calculated value of the activation energy and the preexponential factor present in the usual semiconduction equation [$\sigma=\sigma_0 \exp(-E/2kT)$] was anomalously high for the adsorbed state. A mechanism based on the adsorption-induced reversible structural phase transition in these materials was proposed to be responsible for the appearance of the conductivity peaks as well as for the anomalous conductivity behavior due to adsorption. Studies on the rates of adsorption and desorption of vapors provide[3,4] valuable macroscopic information about the interaction of vapor molecules with the solid surface. It was, therefore, thought worthwhile to examine the rates of adsorption and desorption processes for Fc–H and its derivatives at different cell temperatures within the same working cell temperature region as described in earlier work.[1,2] Interpretation of the results may show the nature of interaction of the vapor molecules with the solid material surface and its variations with temperature. It has already been mentioned in our earlier work[1,2] that in general sensitivity of ethanol vapor is better than other vapors for the adsorption-induced changes in the electrical conductivity of Fc–H and its derivatives. So, systematic experiments were performed mainly with ethanol vapor. The selected cell temperatures are in the different regions of the conductivity vs. temperature plot obtained for ethanol adsorption upon Fc–H[1] and its derivatives.[2] We have already reported the results of such studies for Fc–H.[5] The values of the solid–vapor interaction parameter were estimated by the rate data analysis. Some interesting results regarding the temperature dependence of the interaction parameter were observed. The results of similar investigations in case of some ferrocene derivatives are presented here, alongwith the results of Fc–H, in order to discuss the effect of different substituent groups on the above mentioned solid–vapor interaction parameters.

Experimental

The materials under study are ferrocenecarboxylic acid (Fc–COOH), acetylferrocene (Fc–$COCH_3$), ferrocenecarbaldehyde (Fc–CHO), and benzoylferrocene (Fc–COC_6H_5). High purity microcrystalline materials in powder form were obtained from the Aldrich Chemical Co. (Milwaukee, Wisconsin, U.S.A.). Further purification was done by repeated crystallization. Applying the usual procedure[3,6–8] the conductivity cells were made in air by placing about 10 mg of the fine powder of the materials on a clean stainless steel electrode (plate) in safe light illumination. Two Teflon® spacers, 2 mils (0.00508 cm) thick, were positioned near the edges of the electrode, and the powdered materials were flattened by gently rotating a piece of conducting glass electrode on the top with the conducting side making contact with the specimen. The Teflon® spacers maintained the separation between the electrodes. To maintain the sandwich cell, two spring clips were fixed at a moderate pressure (ca. 0.035 MPa) at the ends of the electrodes.

The cell was placed in a conductivity chamber made of brass and fashioned with Teflon®. All the electrical surface leakage parts were of Teflon®. There was gas inlet and outlet in the conductivity chamber. Chamber atmosphere could circulate freely through the open sides of the sandwich cell. A dc voltage of 27.0 V from dry batteries was applied across the electrodes as a bias potential. The stainless steel electrode was placed inside the chamber on the top of an electrically insulated solid cyllindrical stainless steel rod, bottom portion of which was immersed in a closed constant temperature liquid bath. The desired temperature of this liquid bath, and thereby that of the conductivity cell was controlled by the Proportional Temperature Controller (model no. RTE-110) of Neslab Instruments Inc. (Newington, New Hampshire, U.S.A.). Temperatures were measured by using a copper–constantan thermocouple attached at the top of the metal electrode and a panel meter of Hindusthan Instruments Ltd., India (model no. HIL 2301). Repeated heating and cooling treatments of the sample cell, initially in vacuum and finally in dry nitrogen atmosphere, ensured desorption of water vapor or any other

preadsorbed vapors/gases. Reagent chemicals of spectrograde (E. Merck, B.D.H.) quality were used without further purification; otherwise repeated fractional distillation was performed before use. To allow various vapors inside the chamber, dry nitrogen gas was passed at a constant rate of flow through a bubbler containing the thermostated chemical reagents to maintain a particular vapor pressure of the chemical. All the conductivity measurements were made with an electrometer amplifier EA815 of the Electronic Corporation of India Ltd.

Results and Discussion

On adsorption of a vapor upon the polycrystalline surface of a sample cell, the dark current starts to increase with time and finally attains a saturation value after a certain time. The adsorption process is very fast and in general almost completely reversible. The initial value of the current is reached simply by flushing the chamber with dry nitrogen gas. For a particular material the saturation value of current depends on the vapor pressure and nature of the reacting chemicals used for adsorption, and the sample cell temperature. These are discussed in the following sections.

In Fig. 1, the variation of the dark current of a Fc–COC_6H_5 sample cell with time i.e., adsorption rate due to adsorption of ethanol vapor at different vapor pressures at a sample cell temperature of 299 K is shown. The saturation values of current are found to increase with increasing vapor pressure. When the chamber is flushed with dry nitrogen gas, the vapors start to desorb. Figure 2 represents the rate of desorption for a sample cell of Fc–COC_6H_5 at 299 K for adsorbed ethanol vapor at different pressures. The adsorption and desorption of ethanol vapors in case of Fc–COC_6H_5 were studied for three other cell temperatures (288, 281, and 276 K). Similar investigations were done for the other Fc–H derivatives. It has been observed that the rates of adsorption and desorption of vapors depend on (i) the vapor pressure, (ii) sample cell temperature, and (iii) the nature Fc–H derivatives used. Similar to Fc–H,[5] in case of these derivatives also the enhancements in the dark current in most cases are lower for lower cell temperatures, which is an unusual observation.

It has been observed that the adsorption and desorption rates follow the modified Roginsky–Zeldovich equation[3,8–12] which are as follows:

$$dm/dt = A \exp(-\beta_A m/kT) \quad (1)$$

for adsorption, and

$$-dm/dt = \overset{*}{A} \exp(-\beta_D m/kT) \quad (2)$$

for desorption. Here, m is the amount of vapor adsorbed (or desorbed as applicable) at time t; A, $\overset{*}{A}$, β_A, and β_D are constants at a constant vapor pressure for a particular solid–vapor system; k being the Boltzmann constant and T is the absolute temperature. $\beta_A m$ and $\beta_D m$ give the measure of the activation energy values for adsorption and desorption respectively. For low amount of vapor adsorption, the conductivity after adsorption, at time t, [i.e. $\sigma_A(m)$] follows the relation[3,9]

$$\sigma_A(m) = \sigma_V \exp(\alpha m) \quad (3)$$

where σ_V is the conductivity before adsorption of any vapor; α is a constant. Again, for low amount of vapor adsorption the specific conductivity at equilibrium, $\sigma_A(m_0)$, is given by the relation[3,9]

$$\sigma_A(m_0) = \sigma_V \exp(\alpha Q_0 p) \quad (4)$$

where, m_0 is the amount of vapor adsorbed at equilibrium; p is the vapor pressure; Q_0 is another constant.

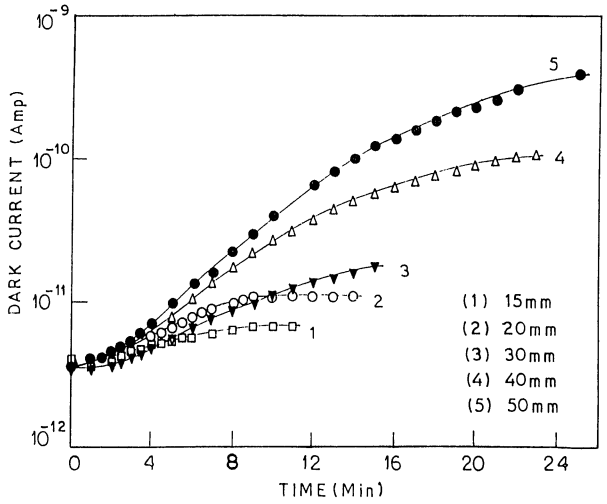

Fig. 1. The change in dark current with time in a powder cell of Fc–COC_6H_5 kept at 299 K after adsorption of ethanol vapor at different vapor pressures (mm=Torr).

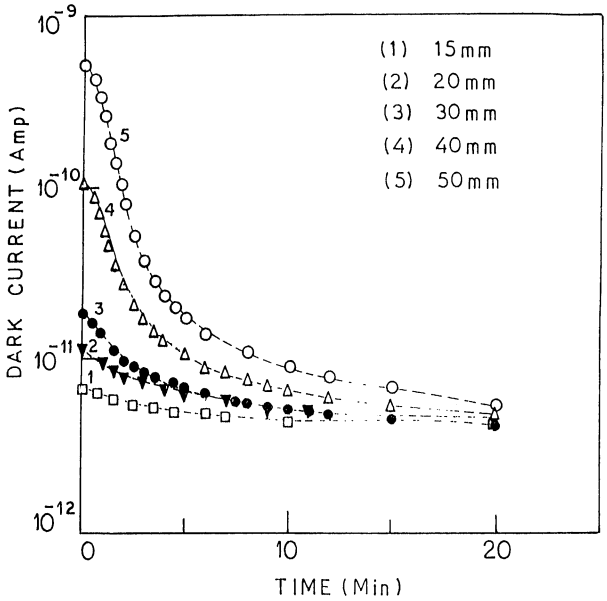

Fig. 2. The change in dark current with time in a powder cell of Fc–COC_6H_5 kept at 299 K during desorption of ethanol vapor at different vapor pressures (mm=Torr).

Integrating Eq. 1 and combining with Eq. 3 we get

$$\log \sigma_A (m) = (\alpha kT/\beta_A) \log (t+t_0) + \text{constant} \quad (5)$$

for adsorption. Similarly for desorption we get

$$\log \sigma_D (m) = (-\alpha kT/\beta_D) \log (t+t_0') + \text{constant} \quad (6)$$

From Eq. 4 a plot of log σ_A (m) [or the logarithm of corresponding current, I] at equilibrium vs. the vapor pressure is expected to be linear. In Fig. 3, such linear plots for ethanol vapor adsorption upon Fc–COC_6H_5 at four different cell temperatures are shown. Thus, the vapor pressure dependence of the saturation current at all the cell temperatures (except 288 K) in case of Fc–COC_6H_5 agrees fairly well with the prediction of Eq. 4. At 288 K the linearity of the plot is observed at lower values of vapor pressure only. In the other Fc–H derivatives the vapor pressure dependence of saturation current is spectacularly cell temperature dependent. For Fc–COOH, farely good linear plots of logarithm of saturation current vs. vapor pressure were observed for the entire vapor pressure range studied for cell temperatures of 285 and 273 K, while the linearity of the above-mentioned plot was restricted to lower vapor pressures for the cell temperature of 299 and 277 K. Similarly, linear plots were observed for the cell temperature of 299 and 276 K for Fc–$COCH_3$ and for 299 and 279 K in case of Fc–CHO for the entire vapor pressure range studied. In other cell temperatures such plots were linear at lower vapor pressures. The deviation from linearity of the plot of logarithm of saturation current vs. vapor pressure at some temperatures indicates that the specific material shows an unusal adsorbing property at those cell temperatures at higher values of vapor pressure. Collins and Mohammed have reported[13] the results for adsorption of NH_3 gas upon nickel phthalocyanine films at different substrate temperatures (350, 326, 311, and 294 K). The current enhancement was found to decrease with increase in temperature at low temperature domain, but this behavior was reversed at 326 K and at 350 K much higher enhancement was observed. The response [response $(R)=\sigma_A(m_0)/\sigma_V$] variation was absolutely substrate temperature dependent, which indicated an unusual adsorbing property at some temperatures, just as has been observed in the present study.

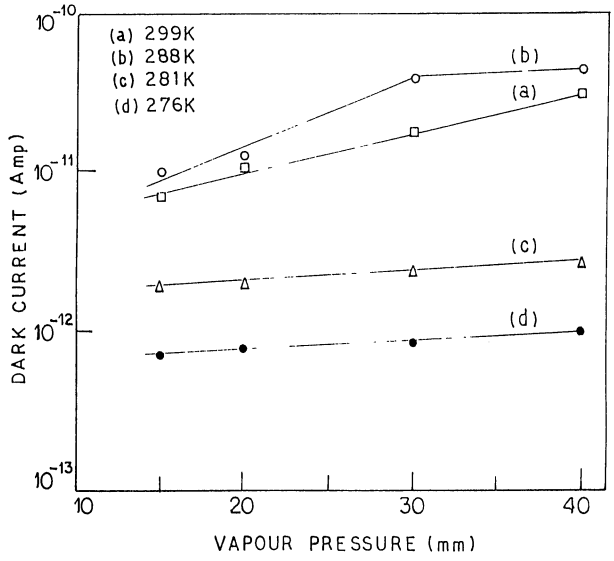

Fig. 3. The change in saturation dark current in a powder cell of Fc–COC_6H_5 as a function of the vapor pressure (mm=Torr) of ethanol vapor at different cell temperatures.

The slopes (αQ_0) of the linear plots of log σ_A (m_0) vs. vapor pressure have been evaluated and are presented in Table 1. The αQ_0 value gives a measure of the interaction between the vapor molecules and solid material surface. In case of Fc–H the variation of the evaluated αQ_0 values (Table 1) for the two lower cell temperatures are quite different from the corresponding values for the two higher cell temperatures. At the lower cell temperatures the value of αQ_0 increases with temperature, while at the two higher cell temperatures this value decreases with temperature. Similar type of temperature dependence of αQ_0 has been observed for Fc–$COCH_3$ and Fc–COC_6H_5 (Table 1). It is interesting to note that a significant change in the value of αQ_0 is observed near the temperature (T_{max}), where a conductivity peak appears in the plot of the measured dark current vs. cell temperature for a sandwich cell of the above-mentioned materials with adsorbed ethanol vapor.[1,2] Though the trend in the variation in αQ_0 with temperature in case of Fc–COOH and Fc–CHO is

Table 1. Cell Temperature Dependence of the Factor αQ_0 for Fc–H and Its Derivatives in Case of Adsorption of Ethanol Vapor

Material	Cell tempeature	Values of αQ_0
	K	mm^{-1} ($\times 10^{-1}$)
Fc–H	299	0.70
	295	1.00
	287	0.63
	276	0.24
Fc–COOH	299	5.60
	285	0.48
	277	2.60
	273	0.43
Fc–$COCH_3$	299	1.23
	290	3.28
	279	0.76
	276	0.20
Fc–CHO	299	2.59
	288	6.71
	279	0.16
	273	1.11
Fc–COC_6H_5	299	0.59
	288	0.95
	281	0.15
	276	0.13

different from the other Fc–H derivatives, a significant change in the value of αQ_0 has been observed at temperatures near T_{max} (Table 1).

It follows from Eqs. 5 and 6 that for any emperically chosen t_0 and t_0',[14] the plots of log σ_A (m) or log I_A (m) vs. log ($t+t_0$) for adsorption and log σ_D (m) or log I_D (m) vs. log ($t+t_0'$) for desorption are expected to be linear, where I_A (m) and I_D (m) are the values of current during adsorption and desorption respectively. Such plots for adsorption at different pressures of ethanol vapor upon a Fc–COC_6H_5 sandwich cell at a temperature of 299 K and also for the corresponding desorption are shown in Fig. 4. Good linear plots, as expected from the (R–Z) Eqs. 5 and 6, are observed from Fig. 4. The time indicated in the abscissa in Fig. 4 is measured from the initiation of adsorption and desorption concerned. The values of $\beta_A/\alpha(=\overset{*}{\beta}_A)$ and β_D/α $(=\overset{*}{\beta}_D)$ at different vapor pressures were evaluated from the slopes of the corresponding R–Z plots in Fig. 4. Similarly the values of $\overset{*}{\beta}_A$ and $\overset{*}{\beta}_D$ at different vapor pressures were calculated from the slopes of the R–Z plots for the other Fc–H derivatives. It should be pointed out here that the R–Z Eqs. 5 and 6 are derived from a combination of the adsorption and desorption rates and Eq. 3. In some cases the data did not follow Eq. 4 [nonlinear cases], hence also Eq. 3, as observed from Fig. 3 (data at 288 K). Therefore, for evaluation of the values of $\overset{*}{\beta}_A$ and $\overset{*}{\beta}_D$ from the slopes of the R–Z plots corresponding to different vapor pressures at various cell temperatures, the nonlinear cases were not considered. As observed in case of many organic semiconducting materials,[3,4,9,15] the $\overset{*}{\beta}_A$ and $\overset{*}{\beta}_D$ values are found to be vapor pressure dependent for a particular cell temperature. From the evaluated values of $\overset{*}{\beta}_A$ and $\overset{*}{\beta}_D$ for different cell temperatures, it is clear that for a fixed vapor pressure the variation of these factors with cell temperature is not a linear one and the variation for different values of vapor pressure is shown in Fig. 5 for Fc–COC_6H_5. As observed from Fig. 5 the change in the $\overset{*}{\beta}_A$ and $\overset{*}{\beta}_D$ values with temperature for Fc–COC_6H_5 in the two lower cell temperatures is quite different from the corresponding change for two higher cell temperatures. The temperature dependence of $\overset{*}{\beta}_A$ and $\overset{*}{\beta}_D$ is reversed around 283 K in case of Fc–COC_6H_5. Similar to the case of Fc–COC_6H_5 in other derivatives also, in most cases, the temperature dependence of $\overset{*}{\beta}_A$ and $\overset{*}{\beta}_D$ is reversed at a certain temperature (depending on the material). It is interesting to note that in case of Fc–CHO, the temperature dependence of $\overset{*}{\beta}_A$ and $\overset{*}{\beta}_D$ as shown in Fig. 6 is different from that of the other Fc–H derivatives (the plot looks like mirror image of the plot presented in Fig. 5). From the temperature depen-

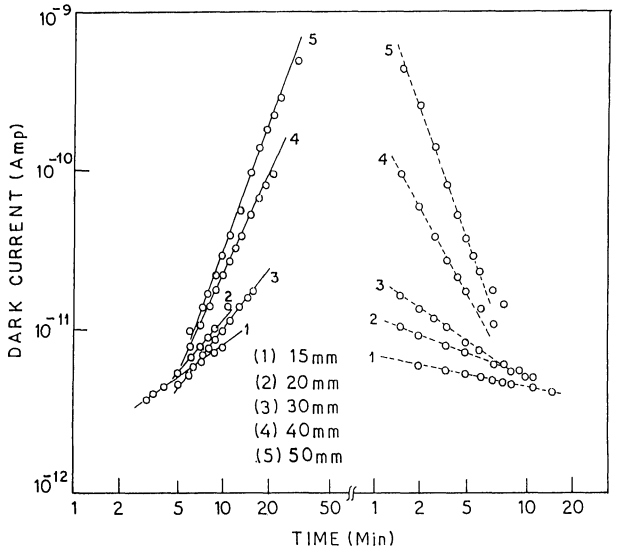

Fig. 4. Adsorption and desorption rates data plotted according to the modified Roginsky–Zeldovich equations for a powder cell of Fc–COC_6H_5 adsorbed with ethanol vapor kept at 299 K. (Solid lines for adsorption and broken lines for desorption) (mm=Torr).

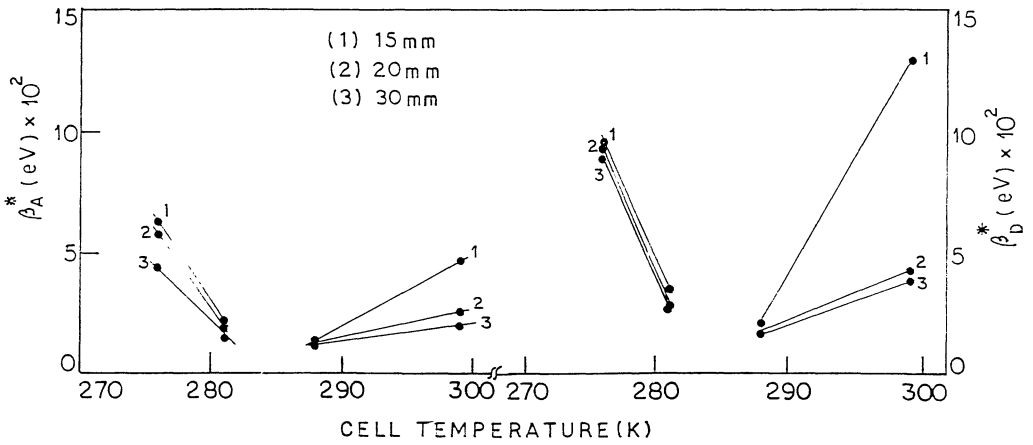

Fig. 5. The change in $\overset{*}{\beta}_A$ and $\overset{*}{\beta}_D$ values with cell temperature for a powder cell of Fc–COC_6H_5 adsorbed with ethanol vapor at different vapor pressures (mm=Torr).

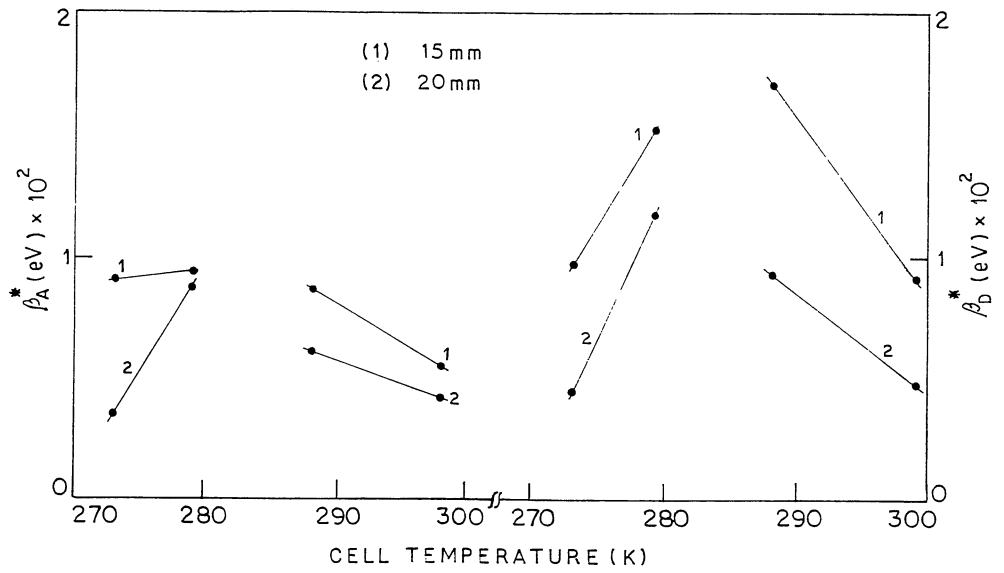

Fig. 6. The change in $\overset{*}{\beta}_A$ and $\overset{*}{\beta}_D$ values with cell temperature for a powder cell of Fc-CHO adsorbed with ethanol vapor at different vapor pressures (mm=Torr).

dence of $\overset{*}{\beta}_A$, $\overset{*}{\beta}_D$, and αQ_0 it is clear that the nature of interaction of vapor molecules with the solid depends drastically on the cell temperature. It is indicated from these results that the interaction is somehow reversed around the temperatures corresponding to the conductivity peaks observed in the plot of the measured dark current vs. cell temperature for a sandwich cell of pure Fc-H derivatives with adsorbed ethanol vapor.[1,2] For example, in case of Fc-COC_6H_5 the reversal appears at around 283 K, the conductivity peak has also been appeared at 283 K. The appearance of conductivity peaks was reported[1,2] to be due to adsorption-induced reversible structural phase transition in these materials. From that results it is expected that the interaction of ethanol vapor molecules with powdery Fc-H derivatives should be reversed around the conductivity peak temperature and this is what has been observed in this present investigation. The exact nature of the adsorption sites (activation centers) and the detailed manner in which the adsorbate vapor molecules are accomodated within the structure of the adsorbent molecules are not known. The experimental results suggest that the distribution of the adsorption sites in these materials is modulated by the adsorption-induced phase transition. Possibly this makes the distribution sites drastically different at different cell temperatures, especially near the phase-transition temperature. As a result, variation of current due to adsorption of a particular vapor (at same pressure) at different cell temperatures near the conductivity peak are significantly different and its effect is reflected in the temperature dependence of $\overset{*}{\beta}_A$, $\overset{*}{\beta}_D$, and αQ_0. It has been pointed out earlier that the adsorption-induced current enhancements were less at lower temperatures. This may be due to the fact that at these temperatures the distribution of adsorption sites in these materials is not favorable for adsorption.

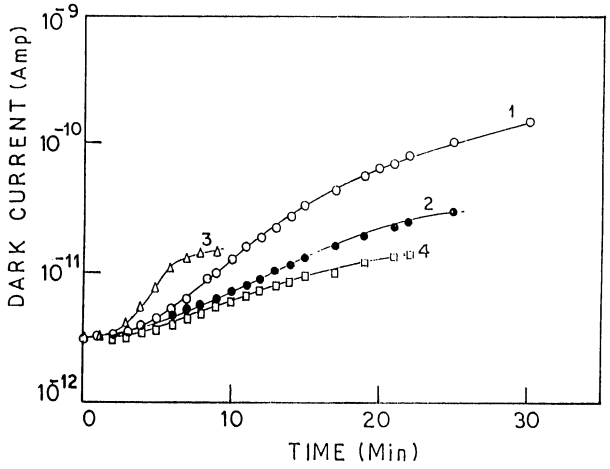

Fig. 7. The change in dark current with time in a powder cell of Fc-COC_6H_5 kept at 299 K after adsorption of different vapors at 40 Torr vapor pressures.
1) 2-Propanol, 2) Methanol, 3) Benzene, 4) Carbon tetrachloride.

Figure 7 represents the variation of the dark current with time due to adsorption of different vapors at same vapor pressure (40 Torr, 1 Torr=133.322 Pa) upon Fc-COC_6H_5 and also the corresponding desorptions (Fig. 8) at a cell temperature of 299 K. Similar measurements have also been done for the other Fc-H derivatives and also measurements were taken at another lower cell temperature for each material. The current enhancement and the rates of adsorption and desorption have been found to be lower at lower cell temperatures for Fc-H. The values of the conductivity enhancement or response [$R=\sigma_A(m_0)/\sigma_V$] for the adsorption of different

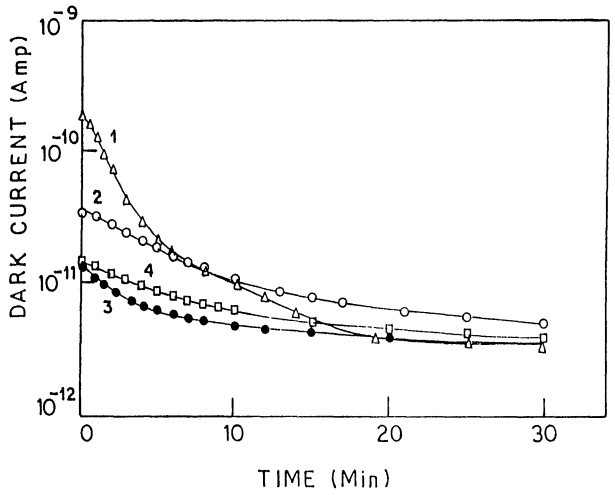

Fig. 8. The change in dark current with time in a powder cell of Fc–COC_6H_5 kept at 299 K during desorption of different vapors at 40 Torr vapor pressures.
1) 2-Propanol, 2) Methanol, 3) Benzene, 4) Carbon tetrachloride.

vapors at 40 Torr vapor pressure upon different materials kept at two different cell temperatures are presented in Table 2. From this table it is clear that the responses of different materials towards a particular vapor differ by a large amount. The responses of a particular material towards different vapors also differ by a large amount. For methanol and carbon tetrachloride vapor adsorption upon Fc–H at 276 K no appreciable change in current was observed. Similarly, methanol vapor shows very poor response to Fc–$COCH_3$. The calculated values of $\overset{*}{\beta}_A$ and $\overset{*}{\beta}_D$ from the slopes of R–Z plots for two different cell temperatures for adsorption of different vapors at same vapor pressure upon Fc–H and its derivatives are shown in Table 3.

The change in the thermodynamic parameters such as entropy and enthalpy occurs as a result of change in vibrational frequencies due to adsorption[17] and will obviously differ from one derivative to another as their molecular structures differ. This provides a possible reason behind the observed differences in the rates of adsorption and desorption of vapors in these materials and the evaluated parameters ($\overset{*}{\beta}_A$, $\overset{*}{\beta}_D$, and αQ_0). Unfortunately, neither the experiment gives any numerical value of α, nor it was possible to measure the amount of vapor adsorbed. The thermodynamic parameters, therefore, could not be estimated.

Fc–H has low ionization potential and so, it is expected to form charge-transfer (CT) complexes with acceptors of medium or strong electron affinity.[18] The observed saturation values of dark current after adsorption of different vapors of same amount bear no linear relationship either with the ionization potential or the electron affinity of the vapors used [the usual test for

Table 2. Values of $R=\sigma_A(m_0)/\sigma_V$ for Adsorption of Different Vapors at 40 Torr Vapor Pressure upon Fc–H and Its Derivatives Kept at Two Different Cell Temperatures

Vapors used	Values of I_p[16]	Values of E_A[1]	Values of D.C.[1] at 298 K	Fc–H		Fc–COOH		Fc–$COCH_3$		Fc–CHO		Fc–COC_6H_5	
				R		R		R		R		R	
	eV	eV		299 K	276 K	299 K	285 K	299 K	276 K	299 K	279 K	299 K	276 K
Methanol	10.84	0.37	32.63	5.9	—[a]	4.6×10^3	4.2×10^5	1.3×10	—[a]	8.9×10	5.3×10^2	4.5	6.6
Ethanol	10.49	0.59	24.30	9.9	1.8	1.8×10^5	2.9×10^5	1.0×10^2	3.5×10	1.9×10^3	5.8×10	7.5	3.6
2-Propanol	10.15	0.67	18.30	3.3×10^3	3.6	1.3×10^5	6.7×10^3	1.1×10^3	3.6×10	1.1×10^4	2.5×10	5.7×10	3.1
Benzene	9.97	2.46	2.27	8.5	2.4	1.2	6.5	3.5	—[a]	1.4×10^2	1.0×10^3	1.0×10	9.7×10
Ethyl acetate	10.11	—	6.02	2.2×10	3.0	2.6	—[a]	—	—	—	—	—	—
Carbon tetrachloride	11.47	1.21	2.23	2.7	—[a]	1.1	—[a]	2.8	—[a]	9.2	1.6×10^2	4.5	1.7×10

a) No appreciable enhancement in the dark current due to adsorption was observed. I_p=ionization potential, E_A=electron affinity, D.C.=dielectric constant.

Table 3. The Values of the Factors $\overset{*}{\beta}_A$ (in eV) and $\overset{*}{\beta}_D$ (in eV) for Fc–H and Its Derivatives in Case of Adsorption of Different Vapors of Same Amount (40 Torr) at Two Cell Temperatures

Vapors used	Fc–H				Fc–COOH				Fc–COCH$_3$				Fc–CHO				Fc–COC$_6$H$_5$			
	$\overset{*}{\beta}_A$ (×10^{-2})		$\overset{*}{\beta}_D$ (×10^{-2})		$\overset{*}{\beta}_A$ (×10^{-2})		$\overset{*}{\beta}_D$ (×10^{-2})		$\overset{*}{\beta}_A$ (×10^{-2})		$\overset{*}{\beta}_D$ (×10^{-2})		$\overset{*}{\beta}_A$ (×10^{-2})		$\overset{*}{\beta}_D$ (×10^{-2})		$\overset{*}{\beta}_A$ (×10^{-2})		$\overset{*}{\beta}_D$ (×10^{-2})	
	299 K	276 K	299 K	276 K	299 K	285 K	299 K	285 K	299 K	276 K	299 K	276 K	299 K	279 K	299 K	279 K	299 K	276 K	299 K	276 K
Benzene	1.9	6.4	4.8	15.2	—[a]	—[a]	—[a]	—[a]	2.9	—[a]	5.9	—[a]	0.7	0.5	0.9	0.9	1.6	0.6	3.1	1.1
Ethyl acetate	1.7	5.8	3.8	13.6	3.0	—[a]	5.8	—[a]	—	—	—	—	—	—	—	—	—	—	—	—
Ethanol	2.1	8.2	4.5	19.0	0.1	0.2	0.2	0.3	1.0	0.8	1.5	1.8	0.2	0.7	0.4	1.0	1.3	3.6	1.6	8.5
2-Propanol	1.3	4.9	3.1	10.0	0.2	0.2	0.5	0.5	0.6	2.0	0.7	2.5	0.3	0.1	0.3	1.6	1.1	3.9	1.6	6.0
Methanol	1.6	—[a]	4.9	—[a]	0.8	0.1	0.3	0.2	0.9	—[a]	2.9	—[a]	0.3	0.4	0.8	0.8	1.3	2.1	4.8	4.6
Carbon tetrachloride	3.7	—[a]	8.8	—[a]	21.9	—[a]	29.5	—[a]	3.3	—[a]	4.4	—[a]	1.3	0.6	3.0	1.0	2.3	0.9	4.7	1.6

a) No appreciable enhancement in the dark current due to adsorption was observed.

CT-complex formation[3,8,19]]. Similar results were obtained for the Fc–H derivatives under investigations also. Thus, the usual test excludes the possibility of the formation of CT-complexes of Fc–H and its derivatives with adsorbed vapors. Change in effective dielectric constant at the adsorbed state is often considered[20] as the reason for the current enhancement in some organic solids due to adsorption. However, the observed non-linear relationship between the static dielectric constant of the vapors used and the saturation values of the dark current after adsorption of the vapors excludes the applicability of this theory of current enhancement. We have reported[1,2] a possible mechanism of charge carrier generation in the adsorbed state considering the adsorption-induced phase transition in Fc–H and its derivatives. Present investigation indicates that the phenomenon of adsorption-induced reversible structural phase transition, which occurs in the adsorbed state of Fc–H and its derivatives may be responsible for the observed temperature dependence of the $\overset{*}{\beta}_A$. $\overset{*}{\beta}_D$, and αQ_0 factors in the case of ethanol adsorption on Fc–H and its derivatives. The observed results show that the value of $\overset{*}{\beta}_A$, $\overset{*}{\beta}_D$, and αQ_0 depend significantly on the nature of the substituent group present at the Fc–H derivatives, but at the present stage it is not possible to correlate the nature of variation of these factors with the substituent group present.

In the adsorption process as the nature of the interaction between the vapor molecule and the solid materials is not well known, there is a need for using experimental techniques that would permit the characterization of the materials at the adsorbed state in the temperature range of interest. Experimental techniques such as surface-enhanced (resonant) Raman scattering (SERS or SERRS) and electronic absorption spectroscopy are powerful analytical techniques[21] that may contribute to characterize and monitor the nature of the interaction between the vapor molecules and the solid materials in the adsorbed state. Unfortunately, such experiments could not be performed due to lack of necessary instrumental facilities.

Thanks are due to Professor T. N. Misra, Head of the Dept. of Specroscopy, I.A.C.S. for his interest in our work.

References

1) B. Mallik and A. Bhattacharjee, *J. Phys. Chem. Solids,* **50**, 1113 (1989).

2) A. Bhattacharjee and B. Mallik, *Bull. Chem. Soc. Jpn.,* **64**, 3129 (1991).

3) B. Mallik, A. Ghosh, and T. N. Misra, *Proc. Indian Acad. Sci., (Chem. Sci.),* **88**, 25 (1979).

4) A. Sarkar, B. Mallik, and T. N. Misra, *J. Phys. Chem. Solids,* **44**, 401 (1983).

5) A. Bhattacharjee and B. Mallik, *J. Phys. Chem. Solids,* **52**, 1187 (1991).

6) T. N. Misra, B. Rosenberg, and R. Switzer, *J. Chem.*

Phys., **48**, 2096 (1968).
7) B. Rosenberg and H. C. Harder, *Photochem. Photobiol.*, **6**, 629 (1967).
8) B. Rosenberg, T. N. Misra, and R. Switzer, *Nature*, **217**, 423 (1968).
9) A. Ghosh, B. Mallik, and T. N. Misra, *Proc. Indian Acad. Sci., (Chem. Sci.)*, **89**, 209 (1980).
10) D.D. Eley and R. B. Leslie, "Advances in Chemical Physics," Interscience Publishing, New York (1964), Vol. 7, p. 238.
11) Ya. Zeldovich, *Acta Physicochim. USSR*, **1**, 449 (1934).
12) S. Roginsky and Ya. Zeldovich, *Acta Physicochim. USSR*, **1**, 554, 595 (1934).
13) R. A. Collins and K. Mohammed, *J. Phys. D: Appl. Phys.*, **21**, 154 (1988).
14) H. A. Taylor and N. Thon, *J. Am. Chem. Soc.*, **74**, 4169 (1952).
15) B. Mitra, D. Sarkar, and T. N. Misra, *J. Phys. Chem. Solids*, **46**, 345 (1985).
16) R. C. Weast, M. J. Astle, and W. H. Beyzer, "CRC Handbook of Chemistry and Physics," 65th ed, CRC Press, Boka Ration, Florida (1984—85), p. E 49.
17) T. A. Kaplan and S. D. Mahanti, *J. Chem. Phys.*, **62**, 100 (1975).
18) R. Foster, "Organic Charge Transfer Complexes," Academic Press, New York (1969), p. 284.
19) B. Mallik, A. Ghosh, and T. N. Misra, *Bull. Chem. Soc. Jpn.*, **52**, 2091 (1979).
20) F. Gutmann and L. E. Lyons, "Organic Semiconductors," Part A," John Wiley, New York (1967), p. 497.
21) D. Battisti and R. Aroca, *J. Am. Chem. Soc.*, **114**, 1201 (1992).